



This discussion paper is/has been under review for the journal Biogeosciences (BG).
Please refer to the corresponding final paper in BG if available.

Multiple stressors of ocean ecosystems in the 21st century: projections with CMIP5 models

L. Bopp¹, L. Resplandy¹, J. C. Orr¹, S. C. Doney⁸, J. P. Dunne², M. Gehlen¹,
P. Halloran³, C. Heinze⁶, T. Ilyina⁴, R. Séférian^{1,5}, J. Tjiputra⁶, and M. Vichi⁷

¹Laboratoire des sciences du climat et de l'environnement (LSCE), IPSL, CEA-UVSQ-CNRS, UMR8212, Gif-sur-Yvette, France

²Geophysical Fluid Dynamics Laboratory, NOAA, Princeton, New Jersey, USA

³Met Office Hadley Centre, Exeter, UK

⁴Max Planck Institute for Meteorology, Bundesstraße 53, 20164 Hamburg, Germany

⁵CNRM-GAME, Météo-France-CNRS, Toulouse, France

⁶Uni Klima, Uni Research, Allégaten 70, 5007 Bergen, Norway

⁷Centro Euro-Mediterraneo sui Cambiamenti Climatici, Istituto Nazionale di Geofisica e Vulcanologia, Bologna, Italy

⁸Woods Hole Oceanographic Institution, Woods Hole, USA

Received: 31 January 2013 – Accepted: 12 February 2013 – Published: 27 February 2013

Correspondence to: L. Bopp (laurent.bopp@lsce.ipsl.fr)

Published by Copernicus Publications on behalf of the European Geosciences Union.

3627

Abstract

Ocean ecosystems are increasingly stressed by human-induced changes of their physical, chemical and biological environment. Among these changes, warming, acidification, deoxygenation and changes in primary productivity by marine phytoplankton can be considered as four of the major stressors of open ocean ecosystems. Due to rising atmospheric CO₂ in the coming decades, these changes will be amplified. Here, we use the most recent simulations performed in the framework of the Coupled Model Intercomparison Project 5 to assess how these stressors may evolve over the course of the 21st century. The 10 Earth System Models used here project similar trends in ocean warming, acidification, deoxygenation and reduced primary productivity for each of the IPCC's representative concentration pathways (RCP) over the 21st century. For the "business-as-usual" scenario RCP8.5, the model-mean changes in 2090s (compared to 1990s) for sea surface temperature, sea surface pH, global O₂ content and integrated primary productivity amount to +2.73 °C, −0.33 pH unit, −3.45% and −8.6%, respectively. For the high mitigation scenario RCP2.6, corresponding changes are +0.71 °C, −0.07 pH unit, −1.81% and −2.0% respectively, illustrating the effectiveness of extreme mitigation strategies. Although these stressors operate globally, they display distinct regional patterns. Large decreases in O₂ and in pH are simulated in global ocean intermediate and mode waters, whereas large reductions in primary production are simulated in the tropics and in the North Atlantic. Although temperature and pH projections are robust across models, the same does not hold for projections of sub-surface O₂ concentrations in the tropics and global and regional changes in net primary productivity.

1 Introduction

Over the past decades, the ocean has undergone large physical and biogeochemical modifications in response to human-induced global change, as revealed by a variety

3628

when compared to our new results, but they all indicate large changes in these marine ecosystem stressors over the coming decades.

Using 13 ocean-only models, Orr et al. (2005) showed that global-mean surface pH could drop by 0.3–0.4 pH unit in 2100 under the IS92a scenario (similar to the RCP8.5 scenario used in our study). In this scenario, Southern Ocean surface waters become undersaturated with respect to aragonite as soon as year 2050. In 2100, aragonite undersaturation extends throughout the entire Southern Ocean and into the subarctic Pacific Ocean.

Coupled climate-marine biogeochemical models used over the past 15 yr all project a long-term decrease in the oceanic O₂ inventory in response to anthropogenic global warming (e.g. Sarmiento et al., 1998; Plattner et al., 2001; Bopp et al., 2002). In a recent intercomparison of seven earth system models, Cocco et al. (2012) found that the oceanic O₂ inventory would decline by 2 to 4% in 2100 under SRES-A2, an earlier IPCC scenario similar to the RCP8.5 scenario used here.

Finally, most coupled climate-marine biogeochemical models also project a decline in NPP in the coming decades as a response to anthropogenic global warming (e.g. Bopp et al., 2001). In a recent model intercomparison study of four coupled models, Steinacher et al. (2010) reported a decrease in global mean NPP of 2–20% by 2100 relative to preindustrial conditions in the SRES A2 emission scenario.

These physical and biogeochemical changes in temperature, pH, O₂ and NPP are known to interact with each other, potentially leading to synergistic effects (Gruber, 2011). Some of these synergistic effects occur at the regional and global scales, one example being the still-debated impact of ocean acidification on ocean deoxygenation. Using ocean biogeochemical models and a simple parameterization based on mesocosm experiments and relating C/N ratios of organic matter to CO₂ levels (Riebesell et al., 2007), Oschlies et al. (2008) and Tagliabue et al. (2011) showed that increasing dissolved CO₂ could induce large increases in sub-surface O₂ utilization, hence expanding the volume of suboxic waters. Synergistic effects also take place at the physiological level. Temperature and dissolved CO₂ may affect levels of tolerance to

3631

low-O₂ concentrations (Pörtner et al., 2004, 2007), whereas elevated CO₂ and lower O₂ levels may reduce thermal tolerance of some organisms (Pörtner 2010; Metzger et al., 2008). These studies emphasize that multiple stressors should be studied together simultaneously in order to be able to evaluate synergistic effects.

Here, we use the most recent simulations performed in the framework of the Coupled Model Intercomparison Project 5 (CMIP5, Taylor et al., 2012) to assess how these stressors may evolve over the course of the 21st century. We focus on four stressors: temperature, pH, O₂ and NPP, while comparing four different representative concentration pathways (RCPs) scenarios across 10 different Earth System Models (ESMs), all including a marine biogeochemical component. The remainder of the paper is organized as follows. Section 2 describes the models and the set of simulations used in this study. Section 3 presents the main results and a discussion, describing major evolution of the different stressors at the global scale, at the regional scale and relations between the stressors. Conclusions and perspectives follow in Sect. 4.

2 Methodology

2.1 Models and simulations

The latest generation of Earth System Models (ESMs) were used to carry out simulations within the framework of CMIP5 (Taylor et al., 2012). These simulations include 4 future scenarios referred to as RCPs (Moss et al., 2010; van Vuuren et al., 2011): RCP8.5, RCP6.0, RCP4.5 and RCP2.6. The RCPs are labeled according to the additional radiative forcing level in 2100 with CO₂ concentrations reaching 936, 670, 538 and 421 ppm respectively. RCP2.6 is also referred to as RCP3PD for “peak and decline”: the atmospheric CO₂ peaks at a concentration of 443 ppm in 2050 before declining in the second half of the 21st century.

The selection of the 10 models used for this study was based on the availability of all variables necessary to discuss the four stressors we focus on, i.e. temperature, pH, O₂

3632

the core analysis by extending it to make use of the full 3-D distribution of temperature, pH and dissolved O₂.

The inter-model difference or model spread is used as an estimate of uncertainty around the projections. To show model agreement on global-mean time-series, we use one inter-model standard deviation. To show model agreement at the regional scale, we use stippling on the maps based on a simple robustness (or agreement) measure. Similar to the approach used for surface temperature changes in Meehl et al. (2007), high robustness for sea surface temperature and for pH is defined when the model-mean simulated change exceeds the inter-model standard deviation (the robustness index, defined as the ratio between model-mean simulated change and inter-model standard deviation is then larger than 1). Similar to the approach used for precipitation changes in Meehl et al. (2007), high robustness for oxygen and NPP is defined when at least 80 % of models agree on the sign of the mean change (robustness index larger than 1). Note that the estimate of uncertainty based on model spread may be biased by an arbitrary distribution of CMIP5 model output for a specific variable and by similarities between models (e.g. IPSL-CM5A-LR and IPSL-CM5A-MR share the same components differ in atmospheric resolution, see Table 1).

2.3 Water mass analysis

We used a global framework to group together water masses of similar behavior. Four classes were defined: Tropical Water (TW) masses, Mode and Intermediate Water (MIW) masses, Deep Water (DW) masses and Bottom Water (BW) masses. For example, the class MIW aims at gathering mode and intermediate waters of all basins, which share common features but are not distributed in the same range of density (Hanawa and Talley, 2001). Limits between classes were defined using several criteria (salinity, stratification, meridional velocities) resulting in different density thresholds in the five different basins (North Atlantic, South Atlantic, North Pacific, South Pacific and Indian Ocean) and for the different models. These density thresholds were computed

3635

for each model using the first ten years (2006–2015) of scenario RCP4.5 (temperature, salinity etc.) and the density referenced to 2000 m (σ_2).

The limit between well stratified TW and homogeneous MIW was defined using a stratification criteria ($\partial\sigma_2/\partial z > 0.02 \text{ kg m}^{-4}$, with z the depth). The lower boundary of MIW was defined as the depth where the salinity is equal to its deep minimum value +0.05. DW were distinguished from BW using the deepest change in sign of meridional velocities, orientated northward in BW and southward in DW. Note that in the North Atlantic MIW are not associated with a deep salinity minimum. Instead the limit between MIW and DW was defined as a minimum in meridional velocities, which are oriented southward in both water masses.

3 Results and discussion

A thorough evaluation, using data-based products, of all simulations used here is beyond the scope of this study. Most models, including their marine biogeochemical components, have been evaluated individually elsewhere (see references in Table 1).

Here, we briefly discuss global mean-values of present day SST, surface pH, oceanic O₂ content and integrated NPP, as listed in Table 2 for each individual model. We also show a regional comparison to data-based products of present-day model-mean SST, surface pH, sub-surface O₂ and NPP (Fig. 1). Finally the skill of the different models in representing spatial and temporal variability of data-based fields are quantified while relying on Taylor diagrams (Taylor, 2001, Fig. 2).

Whereas large-scale patterns are well represented for SST and sub-surface O₂, the comparison to data-based products is much less satisfying for surface pH and NPP (Fig. 1). This is also reflected in the Taylor diagrams, with correlation coefficient (R) ranging from 0.98 to 1.0 for SST, from 0.7 to 0.95 for O₂, but from 0.1 to 0.6 for pH and from 0.2 to 0.6 for NPP (Fig. 2). For NPP, the models score poorly because we do not include the seasonal cycle in the correlation, and (2) they under-represent high productivity in coastal regions. Additionally models that do perform well for one variable

3636

may perform poorly for others (e.g. IPSL-CM5A-MR performs well for NPP ($R \sim 0.6$), but poorly for surface pH ($R \sim 0.2$)).

Global mean values of present-day SST, surface pH, oceanic O₂ content, and integrated NPP also show some striking differences between models, and when compared to observations. This is especially true for the global-averaged O₂ concentration, with some models clearly under-oxygenated (e.g. IPSL-CM5As) and other models over-oxygenated (e.g. NorESM1-ME). For NPP also, some models simulate global integrated values as low as 30.9 PgCyr⁻¹ (IPSL-CMA-MR) whereas others simulate NPP as high as 78.71 PgCyr⁻¹ (GFDL-ESM2M). While these model differences in reproducing present-day patterns and values may explain some of the differences in the model projections we detail below, they also lead us to use relative quantities when comparing NPP changes or O₂ changes, as it is done in the rest of the manuscript.

3.1 Changes of multiple stressors at the global scale

The ocean warms because it takes up much of the additional heat that accumulates in the Earth System from increasing greenhouse gas concentrations. The intensity of simulated sea surface warming in the coming decades is mostly dictated by the RCP scenario, i.e. by the amount of greenhouse gases emitted to the atmosphere, with an inter-model range depending on the strength of the simulated climate feedbacks. From the 1990s to the 2090s, model-mean global average SST increases by +2.73 (± 0.72), +1.58 (± 0.48), +1.28 (± 0.56) and +0.71 (± 0.45) °C for RCP8.5, RCP6.0, RCP4.5 and RCP2.6 respectively (Fig. 3, Table 3). Note that because of our model selection process, these model-mean values would differ from the standard CMIP5 analyses that include a wider selection of models. This simulated increase is, as expected, lower than for global-mean air surface temperature, which amounts to +4.2, +2.5, +1.9 and +1.0 °C for the same 4 RCP scenarios and from 1960–1990 to the end of the 21st century (Knutti and Sedlacek, 2012).

The model spread for each scenario is used as an estimate of uncertainty around the model-mean projection. Part of this model spread is due to internal variability simulated

3637

by the climate models. However, most of it arises from model differences in (1) climate sensitivities (Knutti and Hegerl, 2008) and to (2) the way RCP scenarios are set up, i.e. aerosols and some greenhouse gases concentrations other than CO₂ may differ between models for the same scenario (Szopa et al., 2012). For example, the SST warming for the RCP8.5 scenario reaches +3.5 °C in three of the models (MPI-ESM-LR, IPSL-CM5A-LR and IPSL-CM5A-MR) and only 2.25 °C in two others (GFDL-ESMs) (Fig. 4). This is explained by the differences in climate sensitivity: IPSL-CMs and MPI-ESM-LR have high 2×CO₂ equilibrium climate sensitivities, whereas the GFDL-ESMs are on the low range of climate sensitivities as demonstrated by Andrews et al. (2012b).

Sea surface pH decreases as a consequence of the ocean taking up a significant fraction of anthropogenic carbon accumulated in the atmosphere. Even more than for SST, the magnitude of pH decrease is entirely dictated by the scenario (for a given atmospheric CO₂ concentrations). In the 2090s, the drop in global-average surface pH compared to 1990s values amounts to -0.33 (± 0.003), -0.22 (± 0.002), -0.15 (± 0.001) and -0.07 (± 0.001) pH unit, for RCP8.5, RCP6.0, RCP4.5 and RCP2.6 respectively (Fig. 3, Table 3). The model-mean projection for RCP8.5 is similar to that by Orr et al. (2005) for the IS92a scenario. In this scenario, the surface pH decrease of 0.3–0.4 units by 2100 translates into a 100 to 150 % increase in H⁺ concentration. Simultaneously, carbonate ion concentrations decrease everywhere and eventually reach aragonite undersaturation in the surface waters of the Southern Ocean and the North Pacific (Orr et al., 2005). Even earlier aragonite undersaturation could be reached in the Arctic waters as demonstrated by Steinacher et al. (2009).

In contrast to SST projections, the model spread for global surface pH projections (estimated as the inter-model standard deviation) is very low (less than 0.003 pH unit). This is explained by: (1) the weak interannual variability in global mean surface pH (Fig. 4), (2) a weak climate-pH feedbacks, as demonstrated in Orr et al. (2005) for earlier Earth System Models, (3) the similar carbonate chemistry equations and well-defined constants based on the OCMIP-2 protocol used by most, if not all, models (Orr et al., 2000) and (4) the uniqueness of the ocean acidification forcing, i.e. of

3638

between 1990s and 2090s, and for the two extreme scenarios, RCP8.5 and RCP2.6 respectively. Local model agreement, based on a robustness index detailed in Sect. 2.2, is indicated by stippling.

Changes in SST are not spatially uniform. Stronger warming occurs in the tropics, in the North Pacific and in the Arctic Ocean, with SST increases larger than 4 °C in the RCP8.5 scenario (Fig. 5). On the contrary, much weaker warming, even cooling, is simulated in the North Atlantic and in some parts of the Southern Ocean, where deep convection is strongly reduced or where sea-ice remains unchanged. Robustness of these regional projections is high (Knutti and Sedlacek, 2012), even for the low-emission scenario RCP2.6 (Fig. 6). Only the regions with a weak signal show low robustness, which is a consequence of the signal-to-noise metric used here to estimate robustness (the ratio of model-mean change over inter-model standard deviation).

Changes in surface pH are smoother and more uniform than SST changes, and very robust across models. Surface pH changes range from -0.25 to -0.45 pH unit in RCP8.5 and from -0.05 to -0.15 RCP2.6 (Figs. 5 and 6). Larger changes occur in the surface Arctic Ocean for both scenarios. This is consistent with recent results obtained with the MIROC ESM under the RCP8.5 scenario (Yamamoto et al., 2012). The authors showed that Arctic sea-ice melting amplifies the decrease of surface pH due to the uptake of anthropogenic carbon, consistent with Steinacher et al. (2009).

Changes in sub-surface (200–600 m) O₂ are not spatially uniform and there is less agreement among models. But despite a strong difference in magnitude, the complex patterns of spatial changes are very similar across the two scenarios and reflect the influence of changes in several processes (ventilation, vertical mixing, remineralization) on O₂ levels (Figs. 5 and 6). The North Pacific, the North Atlantic, the Southern Ocean, the subtropical South Pacific and South Indian Oceans all undergo deoxygenation, with O₂ decreases of as much as -50 mmol m⁻³ in the North Pacific for the RCP8.5 scenario. In contrast, the tropical Atlantic and the tropical Indian show increasing O₂ concentrations in response to climate change, in both RCP8.5 and RCP2.6 scenarios. The equatorial Pacific displays a weak east-west dipole, with increasing O₂ in the east

3641

and decreasing O₂ in the west. Apart from changes in the equatorial Pacific, these regional changes in sub-surface O₂ are consistent across models under the RCP8.5 scenario (stippling on Fig. 5), and they are quite similar to those from a recent inter-model comparison of the previous generation of earth system models (Cocco et al., 2012).

Over the mid-latitudes, patterns of projected changes in sub-surface O₂ are broadly consistent with observations collected over the past several decades (Helm et al., 2011; Stendardo and Gruber, 2012; Takatani et al., 2012). Yet there is no such model-data agreement over most of the tropical oceans. Observed time series suggest a vertical expansion of the low-oxygen zones in the eastern tropical Atlantic and the equatorial Pacific during the past 50 yr (Stramma et al., 2008), conversely with models that simulate increasing O₂ levels with global warming over the historical period (Andrews et al., 2012a). A more detailed analysis of the simulated evolution of volumes of low-oxygen waters is given in Sect. 3.2.4.

Similar to sub-surface O₂ and in line with previous modeling studies (Bopp et al., 2001; Steinacher et al., 2010), projected changes in NPP are spatially heterogeneous. A decrease in NPP is consistently simulated across models and scenarios in the tropical Indian Ocean, in the west tropical Pacific, in the tropical Atlantic and in the North Atlantic (Figs. 5 and 6). This decrease reaches as much as -150 g C m⁻² yr⁻¹ regionally in 2090s for the RCP8.5 scenario, more than a 50 % decrease in historical levels of NPP in the North Atlantic, while at the same time there is a 30 % decrease in the tropical Indian and west tropical Pacific. In the eastern equatorial Pacific, the model-mean also indicates a large decrease of NPP, but this response is not consistent across models, with 3 models (GFDL-ESMs and CESM1-BGC) simulating an increase in NPP in response to climate change in that region (eastern Equatorial Pacific). The main mechanisms responsible for NPP decreases in the tropics and in the North Atlantic have been identified in a previous model inter-comparison study (Steinacher et al., 2010) and are linked to a reduced supply of nutrients to the euphotic zone in response to enhanced stratification and slowed circulation.

3642

include temperature-dependent production and remineralization rates, but it is likely that they also use very different parameter values, which would explain the large discrepancy in NPP projections.

Whereas global export production seems to be mostly controlled by the balance between reduction in nutrients supplied to the euphotic layer and alleviation of light and temperature limitations (but also by changes in plankton community as shown by Bopp et al., 2005), larger uncertainties in projections of NPP emphasize the need to improve model representations of more direct biological effects, such as the temperature-dependency of physiological rates studied by Taucher and Oschlies (2011).

3.2.4 Projected changes in the extension of Oxygen Minimum Zones

Oxygen Minimum Zones (OMZs) are key oceanic regions because of their role in the marine nitrogen cycle (water-column denitrification occurs almost exclusively in O_2 -deficient waters) and because of the unusual ecosystems associated with low- O_2 regions (OMZs represent a respiratory barrier for many organisms).

Following Cocco et al. (2012), we used three different thresholds (5, 50 and 80 mmol m^{-3}) to characterize water volumes of low-oxygen waters. Suboxic waters are defined with a threshold of 5 mmol m^{-3} whereas hypoxic waters are defined here with a threshold of 50 mmol m^{-3} . Figure 9 presents the relative evolution of these 3 volumes as simulated by the CMIP5 models over 1870 to 2100 and for the RCP8.5 scenario. Although each model is plotted for each of the three volumes on Fig. 9, we highlight the models for which the simulated volumes over 1990–1999 fall within +100 % and –50 % of the observed volumes (126, 60 and 2.6 millions of km^3 respectively), as estimated from the revised WOA2005 database (Bianchi et al., 2012).

By 2100, all models project an increase in the volume of waters below 80 mmol m^{-3} , ranging from +1 % (MPI-ESMs) to +9 % (CESM1-BGC), relative to 1990–1999. This response is more consistent than that of the previous generation of earth system models, i.e. changes varying from –26 to +16% over 1870 to 2099 under the SRES-A2 scenario (Cocco et al., 2012). Conversely, for lower oxygen levels, there is less

3645

agreement among the CMIP5 models. Simulated volumes do not agree with observations, and changes due to climate change may be either negative or positive. For the volume of waters below 50 mmol m^{-3} , four models project an expansion of 2 % to 16 % (both GFDL-ESMs, HadGEM2-ES and CESM1-BGC), whereas two other models project a slight contraction of ~ 2 % (NorESM1-ME and MPI-ESM-MR). For the volume of waters below 5 mmol m^{-3} , only one model (IPSL-CM5A-MR) is close to the volume estimated from observations and simulates a large expansion of this volume (+30 % in 2090s). These results for low- O_2 waters (5 and 50 mmol m^{-3}) agree with those of Cocco et al. (2012), with large model-data and model-model discrepancies and simulated responses varying in sign for the evolution of these volumes under climate change.

The ability of climate models to represent O_2 observations has been questioned in recent studies. Stramma et al. (2012) used an ESM of intermediate complexity to perform simulations over the historical period and compared the simulated sub-surface O_2 trends with observations. They showed that the model was unable to reproduce the spatial patterns of observed changes. Similarly, Andrews et al. (2012a) compared output of MPI-ESM-LR and HadGEM2-ES to observations over the historical period. They reported that both models fail to reproduce the pattern of O_2 loss recorded by observations in low-latitude OMZs.

A more thorough analysis of the mechanisms responsible for the model-data discrepancies as well as the mechanisms driving the simulated future changes is necessary. Gnanadesikan et al. (2012) performed such an analysis with simulations carried out with a previous version of the GFDL Earth System Model (GFDL-ESM2.1) under the SRES-A2 scenario. They show that the volume of suboxic waters does not increase under global warming in the tropical Pacific. A detailed analysis of the different terms contributing to the O_2 budget showed that an increase in O_2 in very low oxygen waters is associated to an enhanced supply of O_2 through lateral diffusion and increased ventilation along the Chilean coast. These results cast doubt on the ability of the present generation of models to project changes in O_2 accurately at the regional level, especially for low- O_2 waters, and stress the need for more model-data

3646

comparison over the historical period alongside a better understanding of reasons for model biases.

3.3 Relation between stressors and across scenarios

3.3.1 Global scale

5 The existence of potential synergistic effects between the different stressors discussed here emphasizes the need to study them together (Boyd et al., 2008). Figure 10 shows the temporal model-mean evolution of global surface pH, global oxygen content and global NPP versus global sea surface warming for each of the RCPs over 2006–2099. For RCP8.5, all these relationships appear linear, implying a constant fraction of acidification, deoxygenation, and NPP reduction per degree of warming: mean surface pH
10 decreases by 0.127 pH unit $^{\circ}\text{C}^{-1}$, global oxygen content decreases by 1.3% $^{\circ}\text{C}^{-1}$ and global NPP loses 3.3% $^{\circ}\text{C}^{-1}$ (with R^2 of 0.99, 0.99 and 0.95 respectively).

For the other RCPs scenarios, relationships are similar for surface pH vs. SST and for NPP vs. SST, but the relationship breaks down for oxygen content versus sea surface
15 warming (Fig. 10). That is, deoxygenation continues long after sea surface temperatures have stabilized. In particular for the RCP2.6 scenario, the total content of oxygen in the ocean loses an additional 1% in the second half of the 21st century after sea surface warming has been stabilized at $+0.7^{\circ}\text{C}$ in 2050 (Fig. 3). When plotted against heat content change however, a single linear relationship for O_2 content emerges across the
20 different scenarios with a slope of $\sim -0.149\%/10^{22}\text{J}$ or 3.9nmolJ^{-1} ($R^2 > 0.99$) in the RCP8.5 scenario (Fig. 10). This slope of $3.9\text{nmolO}_2\text{J}^{-1}$ is slightly lower than that found in early deoxygenation studies (e.g. 6nmolJ^{-1} in Bopp et al., 2002), but more consistent with the recent study of Frölicher et al. (2009), thus indicating a larger contribution (here around 40%) of warming-induced solubility reduction in global deoxy-
25 genation (which contribution is estimated at 1.5nmolJ^{-1} , Bopp et al., 2002).

3647

3.3.2 Analysis within a water-mass framework

For more insight into regional relationships between the different stressors, we computed trends of temperature, pH and O_2 in distinct water-masses as described in the methodology section. Because coupled climate models have strong biases in the way
5 they simulate the distribution of the main oceanic water masses (see Saltee et al., 2012 for an evaluation of Southern Ocean water masses in the CMIP5 models), this water mass framework is a natural approach to analyze model behavior (Iudicone et al., 2011) or to compare models. Furthermore, it avoids averaging biogeochemical properties between different water masses.

10 Figure 11 details the global relationships between temperature and pH and between temperature and O_2 , respectively, across the different RCP scenarios and for the four distinct water masses (WM).

Not surprisingly, this analysis reveals large differences between the different WM, and for instance between tropical waters (TW) and mode/intermediate waters (MIW).
15 TW are characterized by relatively low acidification-to-warming and low deoxygenation-to-warming ratios (Fig. 11). In contrast, MIW are characterized by much higher acidification- and deoxygenation-to-warming ratios, demonstrating the importance of these water masses in the propagation of the acidification and deoxygenation signals to the ocean's interior. In addition, MIW have a low buffer capacity of the carbonate system thus amplifying the response of pH to the uptake of anthropogenic carbon
20 (see Sect. 3.2.2). The deep and bottom water masses (DW and BW) show very little acidification and warming trends, but some significant deoxygenation trend for the high-emission scenarios (RCP8.5).

The climate change patterns differ when the model results are distinguished by oceanic basin. Figure 12 shows the relationships between pH and temperature, and
25 between O_2 and temperature for 3 of the 4 WMs (omitting TW), averaged over large oceanic basins (North Atlantic, North Pacific and Southern Ocean) for RCP8.5 (2090s minus 2000s). Remarkably, the responses of different stressors in the water masses

3648

O₂-concentrations (and OMZs development) and NPP in some high-productivity regions such as the east Equatorial Pacific.

One critical improvement in future ESMs will be amelioration of biases in the representation of OMZs. A related long term goal will be vastly-enhanced resolution to represent the scales of coastal upwelling and other mesoscale phenomena such as eddies. Finally, representation of ecosystems in models such as these is an evolving science. They represent only a small set of the processes controlling ecosystem and biogeochemical function. While the models are each constructed in mathematically-defensible forms, they are all different in the underlying assumptions. Rather than representing discrete biological forms, they represent ecosystems as a biological continuum with infinite biodiversity in some ways (i.e. the role of temperature), and an artificial rigidity in others (i.e. fixed half saturation constants).

Acknowledgements. We acknowledge the World Climate Research Programme's Working Group on Coupled Modelling, which is responsible for CMIP. For CMIP the US Department of Energy's Program for Climate Model Diagnosis and Intercomparison provides coordinating support and led development of software infrastructure in partnership with the Global Organization for Earth System Science Portals. The authors also thank the IPSL modeling group for the software infrastructure that facilitates CMIP5 analysis. This work was supported through EU FP7 project CARBOCHANGE, EU FP7 project MEECE, and ANR project MACROES. S.C.D. acknowledges the US National Science Foundation (AGS-1048827)..



The publication of this article is financed by CNRS-INSU.

3651

References

- Andrews, O. D., Bindoff, N. L., Halloran, P. R., Ilyina, T., and Le Quéré, C.: Detecting an external influence on recent changes in oceanic oxygen using an optimal fingerprinting method, *Biogeosciences Discuss.*, 9, 12469–12504, doi:10.5194/bgd-9-12469-2012, 2012a.
- Andrews, T., Gregory, J. M., Webb, M. J., and Taylor, K. E.: Forcing, feedbacks and climate sensitivity in CMIP5 coupled atmosphere-ocean climate models, *Geophys. Res. Lett.*, 39, L09712, doi:10.1029/2012GL051607, 2012b.
- Assmann, K. M., Bentsen, M., Segschneider, J., and Heinze, C.: An isopycnic ocean carbon cycle model, *Geosci. Model Dev.*, 3, 143-167, doi:10.5194/gmd-3-143-2010, 2010.
- Aumont, O. and Bopp, L.: Globalizing results from ocean in situ iron fertilization studies, *Global Biogeochem. Cy.*, 20, 1–15, 2006.
- Bates, N. R., Best, M. H. P., Neely, K., Garley, R., Dickson, A. G., and Johnson, R. J.: Detecting anthropogenic carbon dioxide uptake and ocean acidification in the North Atlantic Ocean, *Biogeosciences*, 9, 2509–2522, doi:10.5194/bg-9-2509-2012, 2012.
- Behrenfeld, M. J. and Falkowski, P. G.: Photosynthetic rates derived from satellite-based chlorophyll concentration, *Limnol. Oceanogr.*, 42, 1, 1–20, 1997.
- Behrenfeld, M. J., O'Malley, R. T., Siegel, D. A., McClain, C. R., Sarmiento, J. L., Feldman, G. C., Milligan, A. J., Falkowski, P. G., Letelier, R. M., and Boss, E. S.: Climate-driven trends in contemporary ocean productivity, *Nature*, 444, 752–755, 2006.
- Bentsen, M., Bethke, I., Debernard, J. B., Iversen, T., Kirkevåg, A., Seland, Ø., Drange, H., Roeilandt, C., Seierstad, I. A., Hoose, C., and Kristjánsson, J. E.: The Norwegian Earth System Model, NorESM1-M – Part 1: Description and basic evaluation, *Geosci. Model Dev. Discuss.*, 5, 2843–2931, doi:10.5194/gmdd-5-2843-2012, 2012.
- Bianchi, D., Dunne, J., Sarmiento, J., and Galbraith, E.: Data-based estimates of suboxia, denitrification and N₂O production in the ocean, and their sensitivities to change, *Global Biogeochem. Cy.*, 26, 6550–6555, 2012.
- Bindoff, N., Willebrand, J., Artale, V., Cazenave, A., Gregory, J., Gulev, S., Hanawa, K., Le Quere, C., Levitus, S., Norjiri, Y., Shum, C., Talley, L., and Unnikrishnan, A.: Observations: oceanic climate change and sea level, in: *Climate Change 2007: The Physical Science Basis, Contribution of Working Group I to the Fourth Assessment Report of the Intergovernmental Panel on Climate Change*, edited by: Solomon, S., Qin, D., Manning, M., Chen, Z., Marquis, M., Averyt, K. B., Tignor, M., and Miller, H. L., Tech. Rep., Intergovernmental Panel

3652

on Climate Change, Cambridge University Press, Cambridge, UK and New York, NY, USA, 2007.

- Bopp, L., Monfray, P., Aumont, O., Dufresne, J. L., Le Treut, H., Madec, G., Terray, L., and Orr, J. C.: Potential impact of climate change on marine export production, *Global Biogeochem. Cy.*, 15, 81–99, 2001.
- Bopp, L., Le Quéré, C., Heimann, M., Manning, A. C., and Monfray, P.: Climate-induced oceanic oxygen fluxes: implications for the contemporary carbon budget, *Global Biogeochem. Cy.*, 16, 1022, doi:10.1029/2001GB001445, 2002.
- Boyce, D. G., Lewis, M. R., Worm, B.: Global phytoplankton decline over the past century, *Nature*, 466, 591–96, 2010.
- Boyd, P. W., Doney, S. C., Strzepek, R., Dusenberry, J., Lindsay, K., and Fung, I.: Climate-mediated changes to mixed-layer properties in the Southern Ocean: assessing the phytoplankton response, *Biogeosciences*, 5, 847–864, doi:10.5194/bg-5-847-2008, 2008.
- Cagnazzo, C., Manzini, E., Fogli, P. G., Vichi, M., and Davini, P.: Role of stratospheric dynamics in the ozone-carbon connection in the Southern Hemisphere, *Clim. Dynam.*, submitted, 2013.
- Cocco, V., Joos, F., Steinacher, M., Frölicher, T. L., Bopp, L., Dunne, J., Gehlen, M., Heinze, C., Orr, J., Oschlies, A., Schneider, B., Segschneider, J., and Tjiputra, J.: Oxygen and indicators of stress for marine life in multi-model global warming projections, *Biogeosciences Discuss.*, 9, 10785–10845, doi:10.5194/bgd-9-10785-2012, 2012.
- Doney, S. C.: The growing human footprint on coastal and open-ocean biogeochemistry, *Science*, 328, 1512–1516, 2010.
- Doney, S. C., Lima, I., Moore, J. K., Lindsay, K., Behrenfeld, M. J., Westberry, T. K., Mahowald, N., Glover, D. M., and Takahashi, T.: Skill metrics for confronting global upper ocean ecosystem-biogeochemistry models against field and remote sensing data, *J. Marine Syst.*, 76, 95–112, 2009.
- Doney, S. C., Ruckelshaus, M., Duffy, J. E., Barry, J. P., Chan, F., English, C. A., Galindo, H. M., Grebmeier, J. M., Hollowed, A. B., Knowlton, N., Polovina, J., Rabalais, N. N., Sydeman, W. J., and Talley, L. D.: Climate change impacts on marine ecosystems, *Annu. Rev. Mar. Sci.*, 4, 11–37, 2012.
- Dore, J. E., Lukas, R., Sadler, D. W., Church, M. J., and Karl, D. M.: Physical and biogeochemical modulation of ocean acidification in the central North Pacific, *P. Natl. Acad. Sci. USA*, 106, 12235–12240, 2009.

3653

- Dufresne, J.-L., Foujols, M.-A., Denvil, S., Caubel, A., Marti, O., Aumont, O., Balkanski, Y., Bekki, S., Bellenger, H., Benshila, R., Bony, S., Bopp, L., Braconnot, P., Brockmann, P., Cadule, P., Cheruy, F., Codron, F., Cozic, A., Cugnet, D., de Noblet, N., Duvel, J.-P., Ethé, C., Fairhead, L., Fichefet, T., Flavoni, S., Friedlingstein, P., Grandpeix, J.-Y., Guez, L., Guilyardi, E., Hauglustaine, D., Hourdin, F., Idelkadi, A., Ghattas, J., Jousseaume, S., Kageyama, M., Krinner, G., Labetoulle, S., Lahellec, A., Lefebvre, M.-P., Lefevre, F., Levy, C., Li, Z. X., Lloyd, J., Lott, F., Madec, G., Mancip, M., Marchand, M., Masson, S., Meurdesoif, Y., Mignot, J., Musat, I., Parouty, S., Polcher, J., Rio, C., Schulz, M., Swingedouw, D., Szopa, S., Talandier, C., Terray, P., and Viovy, N.: Climate change projections using the IPSL-CM5 Earth System Model: from CMIP3 to CMIP5, *Clim Dynam.*, accepted, 2013.
- Dunne, J. P., John, J., Adcroft, A., Griffies, S. M., Hallberg, R. W., Shevliakova, E., Stouffer, R. J., Cooke, W. F., Dunne, K. A., Harrison, M. J., Krasting, J. P., Malyshev, S., Milly, P. C. D., Philipps, P., Sentman, L. T., Samuels, B. L., Spelman, M. J., Winton, M., Wittenberg, A. T., and Zadeh, N.: GFDL's ESM2 global coupled climate-carbon Earth System Models Part I: Physical formulation and baseline simulation characteristics, *J. Climate*, 25, 6646–6665, doi:10.1175/JCLI-D-11-00560.1, 2012a.
- Dunne, J. P., John, J. G., Shevliakova, E., Stouffer, R. J., Krasting, J. P., Malyshev, S., Milly, P. C. D., Sentman, L. T., Adcroft, A., Cooke, W. F., Dunne, K. A., Griffies, S. M., Hallberg, R. W., Harrison, M. J., Levy II, H., Wittenberg, A. T., Philipps, P., and Zadeh, N.: GFDL's ESM2 global coupled climate-carbon Earth System Models Part II: Carbon system formulation and baseline simulation characteristics, *J. Climate*, doi:10.1175/JCLI-D-12-00150.1, 2012b.
- Friedlingstein P., Meinshausen, M., Arora, V. K., Jones, C. D., Liddicoat S. K., Knutti, R.: CMIP5 climate projections and uncertainties due to carbon cycle feedbacks, *J. Climate*, in review, 2013.
- Frölicher, T. L., Joos, F., Plattner, G. K., Steinacher, M., and Doney, S. C.: Natural variability and anthropogenic trends in oceanic oxygen in a coupled carbon cycle-climate model ensemble, *Global Biogeochem. Cy.*, 23, GB1003, doi:10.1029/2008GB003316, 2009.
- Gent, P. R., Danabasoglu, G., Donner, L. J., Holland, M. M., Hunke, E. C., Jayne, S. R., Lawrence, D. M., Neale, R. B., Rasch, P. J., Vertenstein, M., Worley, P. H., Yang, Z.-L., and Zhang, M.: The community climate system model version 4, *J. Climate*, 24, 4973–4991, 2011.

3654

- Gilbert, D., Rabalais, N. N., Díaz, R. J., and Zhang, J.: Evidence for greater oxygen decline rates in the coastal ocean than in the open ocean, *Biogeosciences*, 7, 2283–2296, doi:10.5194/bg-7-2283-2010, 2010.
- 5 Giorgetta, M. A., Jungclaus, J. H., Reick, C. H., Legutke, S., Brovkin, V., Crueger, T., Esch, M., Fieg, K., Glushak, K., Gayler, V., Haak, H., Hollweg, H.-D., Ilyina, T., Kinne, S., Kornblueh, L., Matei, D., Mauritsen, T., Mikolajewicz, U., Mueller, W. A., Notz, D., Raddatz, T., Rast, S., Redler, R., Roeckner, E., Schmidt, H., Schnur, R., Segschneider, J., Six, K., Stockhause, M., Wegner, J., Widmann, H., Wieners, K.-H., Claussen, M., Marotzke, J., and Stevens, B.: Climate change from 1850 to 2100 in MPI-ESM simulations for the Coupled Model Intercomparison Project 5, submitted, 2013.
- 10 Gnanadesikan, A., Dunne, J. P., and John, J.: Understanding why the volume of suboxic waters does not increase over centuries of global warming in an Earth System Model, *Biogeosciences*, 9, 1159–1172, doi:10.5194/bg-9-1159-2012, 2012.
- Gruber, N.: Warming up, turning sour, losing breath: ocean biogeochemistry under global change, *Philos. T. R. Soc. A*, 369, 1980–1996, 2011.
- 15 Hanawa, K. and Talley, L. D.: Mode waters, in: *Ocean Circulation and Climate*, edited by: Siedler, G. and Church, J., International Geophysics Series, Academic Press, 373–386, 2001.
- Helm, K. P., Bindoff, N. L., and Church, J. A.: Observed decreases in oxygen content of the global ocean, *Geophys. Res. Lett.*, 38, L23602, doi:10.1029/2011GL049513, 2011.
- 20 Henson, S. A., Sarmiento, J. L., Dunne, J. P., Bopp, L., Lima, I., Doney, S. C., John, J., and Beaulieu, C.: Detection of anthropogenic climate change in satellite records of ocean chlorophyll and productivity, *Biogeosciences*, 7, 621–640, doi:10.5194/bg-7-621-2010, 2010.
- Hofmann, G. E., Barry, J. P., Edmunds, P. J., Gates, R. D., Hutchins, D. A., Klinger, T., and Sewell, M. A.: The effects of ocean acidification on calcifying organisms in marine ecosystems: an organism to ecosystem perspective, *Annu. Rev. Ecol. Evol. S.*, 41, 127–47, 2010.
- 25 Hutchins, D. A., Fu, F.-X., Zhang, Y., Warner, M. E., Feng, Y., Portune, K., Bernhardt, P. W., and Mulholland, M. R.: CO₂ control of *Trichodesmium* N₂ fixation, photosynthesis, growth rates, and elemental ratios: Implications for past, present, and future ocean biogeochemistry, *Limnol. Oceanogr.*, 52, 1293–1304, 2007.
- 30 Ilyina, T., Six, K. D., Segschneider, J., Maier-Reimer, E., Li, H., and Nunez-Riboni, I.: The global ocean biogeochemistry model HAMOCC: Model architecture and performance as compo-

3655

- ment of the MPI-Earth System Model in different CMIP5 experimental realizations, submitted, 2013.
- 5 Ishii, M., Ishii, M., Inoue, H. Y., Midorikawa, T., Saito, S., Tokieda, T., Sasano, D., Nakadate, A., Nemoto, K., Metz, N., Wong, C. S., and Feely, R. A.: Spatial variability and decadal trend of the oceanic CO₂ in the western equatorial Pacific warm/fresh water, *Deep-Sea Res. Pt. II*, 56, 591–606, 2009.
- Iudicone, D., Rodgers, K. B., Stendardo, I., Aumont, O., Madec, G., Bopp, L., Mangoni, O., and Ribera d'Alcala', M.: Water masses as a unifying framework for understanding the Southern Ocean Carbon Cycle, *Biogeosciences*, 8, 1031–1052, doi:10.5194/bg-8-1031-2011, 2011.
- 10 Jones C. D., Robertson, E., Arora, V., Friedlingstein, P., Shevliakove, E., Bopp, L., Brovkin, V., Hajima, T., Kato, E., Kawamiya, M., Liddicoat, S., Lindsay, K., Reick, C., Roelandt, C., Segschneider, J., Tjiputra, J.: 21st Century compatible CO₂ emissions and airborne fraction simulated by CMIP5 Earth System models under 4 Representative Concentration Pathways, *J. Climate*, in press, 2013.
- 15 Keeling, R. F., Körtzinger, A., and Gruber, N.: Ocean deoxygenation in a warming world, *Annu. Rev. Mar. Sci.*, 2, 199–229, doi:10.1146/annurev.marine.010908.163855, 2010.
- Knutti, R. and Hegerl, G. C.: The equilibrium sensitivity of the Earth's temperature to radiation changes, *Nat. Geosci.*, 1, 735–743, doi:10.1038/ngeo337, 2008.
- Knutti, R. and Sedlacek, J.: Robustness and uncertainties in the new CMIP5 climate model projections, *Nat. Clim. Change*, doi:10.1038/nclimate1716, 2012.
- 20 Lindsay, K., Bonan, G. B., Doney, S.C., Hoffmann, F. M., Lawrence, D. M., Long, M. C., Mahowald, N. M., Moore, J. K., Randerson, J. T., and Thornton, P. E.: Preindustrial control and 20th century carbon cycle experiments with the earth system model CESM1-(BGC), *J. Climate*, submitted, 2013.
- 25 Meehl, G. A., Stocker, T. F., Collins, W. D., Friedlingstein, P., Gaye, A. T., Gregory, J. M., Kitoh, A., Knutti, R., Murphy, J. M., Noda, A., Raper, S. C. B., Watterson, I. G., Weaver, A. J., and Zhao, Z.-C.: *Climate Change 2007: The Physical Science Basis. Contribution of Working Group I to the Fourth Assessment Report of the Intergovernmental Panel on Climate Change*, chap. Global Climate Projections, Cambridge University Press, Cambridge, UK and New York, NY, USA, 747–846, 2007.
- 30 Metzger, R., Sartoris, F. J., Langenbuch, M., and Pörtner, H. O.: Influence of elevated CO₂ concentrations on thermal tolerance of the edible crab cancer pagurus, *J. Therm. Bio.*, 32, 144–151, doi:10.1016/j.jtherbio.2007.01.010, 2007.

3656

- Moore, J. K., Doney, S. C., Kleypas, J. A., Glover, D. M., and Fung, I. Y.: An intermediate complexity marine ecosystem model for the global domain, *Deep-Sea Res. Pt. II*, 49, 403–462, doi:10.1016/S0967-0645(01)00108-4, 2002.
- Moore, J. K., Doney, S. C., and Lindsay, K.: Upper ocean ecosystem dynamics and iron cycling in a global 3-D model, *Global Biogeochem. Cy.*, 18, GB4028, doi:10.1029/2004GB002220, 2004.
- Moss, R. H., Edmonds, J. A., Hibbard, K. A., Manning, M. R., Rose, S. K., van Vuuren, D. P., Carter, T. R., Emori, S., Kainuma, M., Kram, T., Meehl, G. A., Mitchell, J. F. B., Nakicenovic, N., Riahi, K., Smith, S. J., Stouffer, R. J., Thomson, A. M., Weyant, J. P., and Wilbanks, T. J.: The next generation of scenarios for climate change research and assessment, *Nature*, 463, 747–756, 2010.
- Nixon, S. and Thomas, A.: On the size of the Peru upwelling ecosystem, *Deep-Sea Res Pt. I*, 48, 2521–2528, 2001.
- Orr, J. C.: Future changes in ocean carbonate chemistry in: *Ocean Acidification*, edited by: Gattuso, J.-P. and Hansson, L., Oxford University Press, 2011.
- Orr, J., Fabry, V., Aumont, O., Bopp, L., Doney, S., Feely, R., Gnanadesikan, A., Gruber, N., Ishida, A., Joos, F., Key, R., Lindsay, K., Maier-Reimer, E., Matear, R., Monfray, P., Mouchet, A., Najjar, R., Plattner, G., Rodgers, K., Sabine, C., Sarmiento, J., Schlitzer, R., Slater, R., Totterdell, I., Weirig, M., Yamanaka, Y., and Yool, A.: Anthropogenic ocean acidification over the twenty-first century and its impact on calcifying organisms, *Nature*, 437, 681–686, 2005.
- Oschlies, A., Schulz, K. G., Riebesell, U., and Schmittner, A.: Simulated 21st century's increase in oceanic suboxia by CO₂-enhanced biotic carbon export, *Global Biogeochem. Cy.*, 22, GB4008, doi:10.1029/2007GB003147, 2008.
- Palmer, J. R. and Totterdell, I. J.: Production and export in a global ecosystem model, *Deep-Sea Res. Pt. I*, 48, 1169–1198, 2001.
- Patara L., Vichi, M., and Masina, S.: Impacts of natural and anthropogenic climate variations on North Pacific plankton in an Earth System Model, *Ecol. Model.*, 244, 132–147, doi:10.1016/j.ecolmodel.2012.06.012, 2012.
- Paulmier, A. and Ruiz-Pino, D.: Oxygen minimum zones (OMZs) in the modern ocean, *Prog. Oceanogr.*, 80, 113–128, 2009.
- Pauly, D. and Christensen, V.: Primary production required to sustain global fisheries, *Nature*, 374, 255–257, 1995.

3657

- Plattner, G., Joos, F., and Stocker, T.: Revision of the global carbon budget due to changing air-sea oxygen fluxes, *Global Biogeochem. Cy.*, 16, 1096–1108, doi:10.1029/2001GB001746, 2002.
- Polovina, J. J., Howell, E. A., and Abecassis, M.: Ocean's least productive waters are expanding, *Geophys. Res. Lett.*, 35, L03618, doi:10.1029/2007GL031745, 2008.
- Pörtner, H. O.: Ecosystem effects of ocean acidification in times of ocean warming: a physiologist's view, *Mar. Ecol. Prog. Ser.*, 373, 203–217, 2008.
- Pörtner, H. O.: Oxygen and capacity limitation of thermal tolerance: a matrix for integrating climate related stressors in marine ecosystems, *J. Exp. Bio.*, 213, 881–893, hdl:10013/epic.34353, 2010.
- Pörtner, H. O. and Knust, R.: Climate change affects marine fishes through the oxygen limitation of thermal tolerance, *Science*, 315, 95–97, doi:10.1126/science.1135471, 2007.
- Pörtner, H. O., Langenbuch, M., and Michaelidis, B.: Synergistic effects of temperature extremes, hypoxia, and increases in CO₂ on marine animals: from Earth history to global change, *J. Geophys. Res.*, 110, C09S10, doi:10.1029/2004JC002561, 2004.
- Resplandy, L., Bopp L., Orr, J. C., and Dunne J. P.: Role of mode and intermediate waters in future ocean acidification: analysis of CMIP5 models, *Geophys. Res. Lett.*, submitted, 2013.
- Rykaczewski, R. R. and Dunne, J. P.: Enhanced nutrient supply to the California Current Ecosystem with global warming and increased stratification in an earth system model, *Geophys. Res. Lett.*, 37, L21606, doi:10.1029/2010GL045019, 2010.
- Rykaczewski, R. R. and Dunne, J. P.: A measured look at ocean chlorophyll trends, *Nature*, 472, E5–E6, doi:10.1038/nature09952, 2011.
- Riebesell, U., Schulz, K. G., Bellerby, R. G. J., Botros, M., Fritsche, P., Meyerhofer, M., Neill, C., Nondal, G., Oschlies, A., Wohlers, J., and Zollner, E.: Enhanced biological carbon consumption in a high CO₂ ocean, *Nature*, 450, 545–548, 2007.
- Sabine, C. L., Feely, R. A., Gruber, N., Key, R. M., Lee, K., Bullister, J. L., Wanninkhof, R., Wong, C. S., Wallace, D. W. R., Tilbrook, B., Millero, F. J., Peng, T.-H., Kozyr, A., Ono, T., and Rios, A. F.: The oceanic sink for anthropogenic CO₂, *Science*, 305, 367–371, 2004.
- Sallée, J. B., Shuckburgh, E., Bruneau, N., Meijers, A., Wang, Z., and Bracegirdle, T.: Assessment of Southern Ocean water mass circulation in CMIP5 models: historical bias and forcing response, *J. Geophys. Res.*, submitted, 2012.
- Sarmiento, J. L., Hughes, T. M. C., Stouffer, R. J., and Manabe, S.: Simulated response of the ocean carbon cycle to anthropogenic climate warming, *Nature*, 393, 245–249, 1998.

3658

- Schmittner, A., Oschlies, A., Matthews, H. D., and Galbraith, E. D.: Future changes in climate, ocean circulation, ecosystems, and biogeochemical cycling simulated for a business-as-usual CO₂ emission scenario until year 4000 AD, *Global Biogeochem. Cy.*, 22, GB1013, doi:10.1029/2007GB002953, 2008.
- 5 Steinacher, M., Joos, F., Frölicher, T. L., Plattner, G.-K., and Doney, S. C.: Imminent ocean acidification in the Arctic projected with the NCAR global coupled carbon cycle-climate model, *Biogeosciences*, 6, 515–533, doi:10.5194/bg-6-515-2009, 2009.
- Steinacher, M., Joos, F., Frölicher, T. L., Bopp, L., Cadule, P., Cocco, V., Doney, S. C., Gehlen, M., Lindsay, K., Moore, J. K., Schneider, B., and Segschneider, J.: Projected 21st century decrease in marine productivity: a multi-model analysis, *Biogeosciences*, 7, 979–1005, doi:10.5194/bg-7-979-2010, 2010.
- 10 Stendero, I. and Gruber, N.: Oxygen trends over five decades in the North Atlantic, *J. Geophys. Res.*, 117, C11004, doi:10.1029/2012JC007909, 2012.
- Stramma, L., Johnson, G. C., Sprintall, J., and Mohrholz, V.: Expanding oxygen-minimum zones in the tropical oceans, *Science*, 320, 655–658, doi:10.1126/science.1153847, 2008.
- 15 Stramma, L., Oschlies, A., and Schmidtko, S.: Anticorrelated observed and modeled trends in dissolved oceanic oxygen over the last 50 years, *Biogeosciences Discuss.*, 9, 4595–4626, doi:10.5194/bgd-9-4595-2012, 2012.
- Szopa, S., Balkanski, Y., Schulz, M., Bekki, S., Cugnet, D., Fortems-Cheiney, A., Turquety, S., Cozic, A., Déandres, C., Hauglustaine, D., Idelkadi, A., Lathière, J., Lefevre, F., Marchand, M., Vuolo, R., Yan, N., and Dufresne, J.-L.: Aerosol and ozone changes as forcing for climate evolution between 1850 and 2100, *Clim. Dynam.*, doi:10.1007/s00382-012-1408-y, 2012.
- 20 Takatani, Y., Sasano, D., Nakano, T., Midorikawa, T., and Ishii, M.: Decrease of dissolved oxygen after the mid-1980s in the western North Pacific subtropical gyre along the 137° E repeat section, *Global Biogeochem Cy.*, 26, GB2013, doi:10.1029/2011GB004227, 2012.
- 25 Taylor, K. E.: Summarizing multiple aspects of model performance in a single diagram, *J. Geophys. Res.*, 106, 7183–7192, 2001.
- Taylor, K. E., Stouffer, R. J., and Meehl, G. A.: An overview of CMIP5 and the experiment design, *B. Am. Meteorol. Soc.*, 93, 485–498, doi:10.1175/BAMS-D-11-00094.1, 2012.
- 30 Thomas, M. K., Kremer, C. T., Klausmeier, C. A., and Litchman, E.: A global pattern in thermal adaptation in marine phytoplankton, *Science*, 338, 1085–1088, doi:10.1126/science.1224836, 2012.

3659

- Tagliabue, A., Bopp, L., and Gehlen, M.: The response of marine carbon and nutrient cycles to ocean acidification: large uncertainties related to phytoplankton physiological assumptions, *Global Biogeochem. Cy.*, 25, GB3017, doi:10.1029/2010GB003929, 2011.
- 5 Taucher, J. and Oschlies, A.: Can we predict the direction of marine primary production change under global warming?, *Geophys. Res. Lett.*, 38, L02603, doi:10.1029/2010GL045934, 2011.
- van Vuuren, D. P., Edmonds, J., Kainuma, M., Riahi, K., Thomson, A., Hibbard, K., Hurtt, G. C., Kram, T., Krey, V., Lamarque, J.-F., Masui, T., Meinshausen, M., Nakicenovic, N., Smith, S. J., and Rose, S. K.: The representative concentration pathways: an overview, *Climatic Change*, 109, 5–31, doi:10.1007/s10584-011-0148-z, 2011.
- 10 Vichi, M., Pinardi, N., and Masina, S.: A generalized model of pelagic biogeochemistry for the global ocean ecosystem. Part I: Theory, *J. Marine Syst.*, 64, 89–109, doi:10.1016/j.jmarsys.2006.03.006, 2007.
- Vichi, M., Manzini, E., Fogli, P. G., Alessandri, A., Patara, L., Scoccimarro, E., Masina, S., and Navarra, A.: Global and regional ocean carbon uptake and climate change: sensitivity to a substantial mitigation scenario, *Clim. Dynam.*, 37, 1929–1947, doi:10.1007/s00382-011-1079-0, 2011.
- 15 Yamamoto, A., Kawamiya, M., Ishida, A., Yamanaka, Y., and Watanabe, S.: Impact of rapid sea-ice reduction in the Arctic Ocean on the rate of ocean acidification, *Biogeosciences*, 9, 2365–2375, doi:10.5194/bg-9-2365-2012, 2012.
- 20

3660

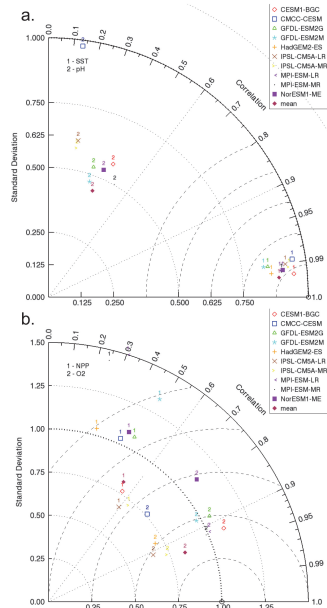


Fig. 2. Taylor diagrams showing the correspondence between model results and observations for **(a)** annual-mean SST and annual-mean surface pH, and **(b)** annual mean sub-surface O₂ averaged over 200–600 m and annual-mean vertically integrated NPP. Data-based products are from Reynolds et al. (2008) for SST, computed using DIC and alkalinity from Key et al. (2004) for surface pH, from WOA (2009) for dissolved O₂ concentrations, from Behrenfeld et al. (1997) for NPP. All data are from 1990–1999 except observed NPP from 1997–2006, and O₂ concentration from WOA 2009 climatology. The angular coordinate indicates the correlation coefficient (R), the radial coordinate shows the normalised standard deviation ($\text{std}_{\text{model}}/\text{std}_{\text{obs}}$). A model perfectly matching the observations would reside in point (1,1).

3665

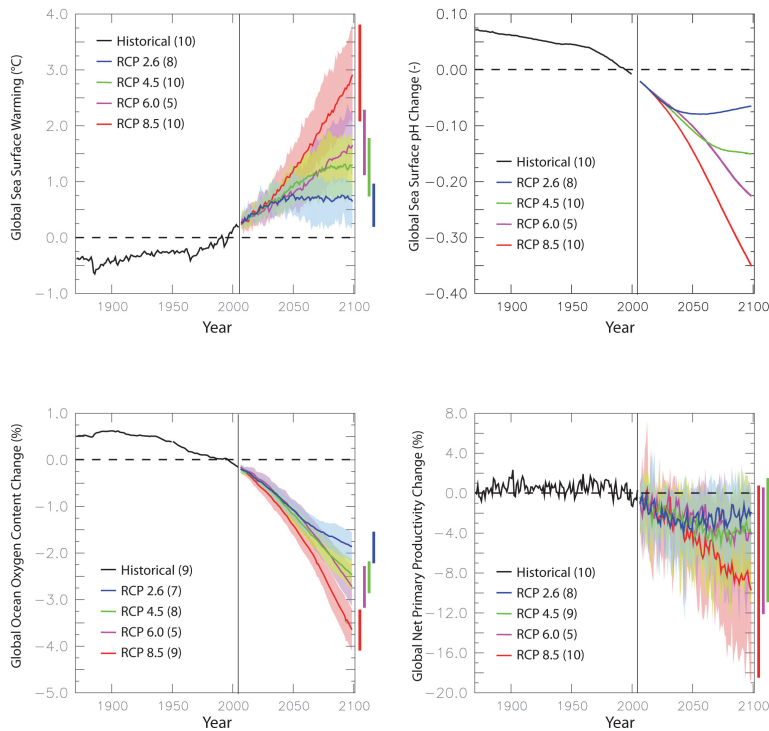


Fig. 3. Model-mean time series of global sea surface warming (°C), surface pH change (pH unit), ocean O₂ content change (%), and global NPP change (%) over 1870–2100 using historical simulations as well as all RCPs simulations. Shading indicates one inter-model standard deviation. All variables are plotted relative to 1990–1999.

3666

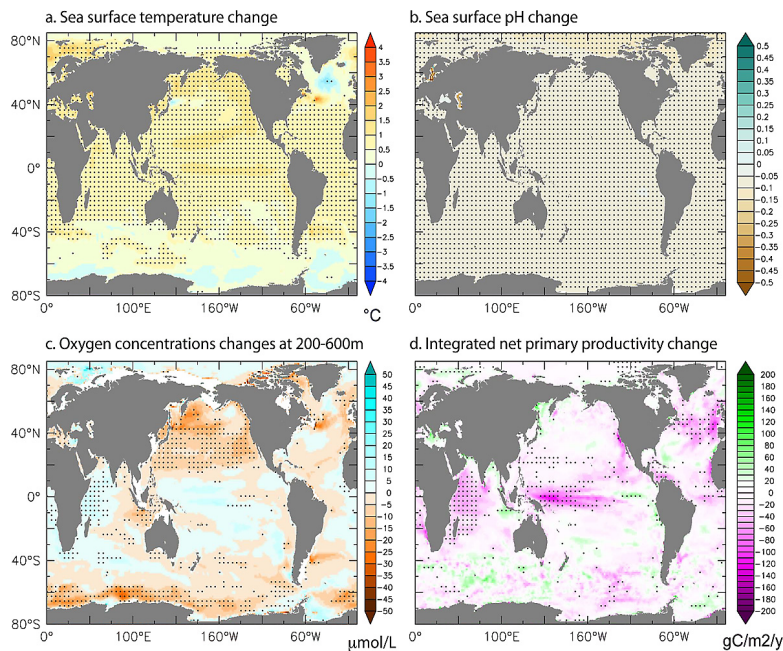


Fig. 6. Change in stressor intensity in 2090–2099 relative to 1990–1999 under RCP2.6. Multi-model mean of (a) sea surface warming ($^{\circ}\text{C}$), (b) surface pH change (pH unit), (c) sub-surface dissolved O_2 concentrations change (averaged between 200 m and 600 m, mmol m^{-3}), and (d) vertically integrated NPP ($\text{gC m}^{-2} \text{yr}^{-1}$). Stippling marks high robustness. Robustness is estimated from inter-model standard deviation for SST and pH, from agreement on sign of changes for O_2 and NPP.

3669

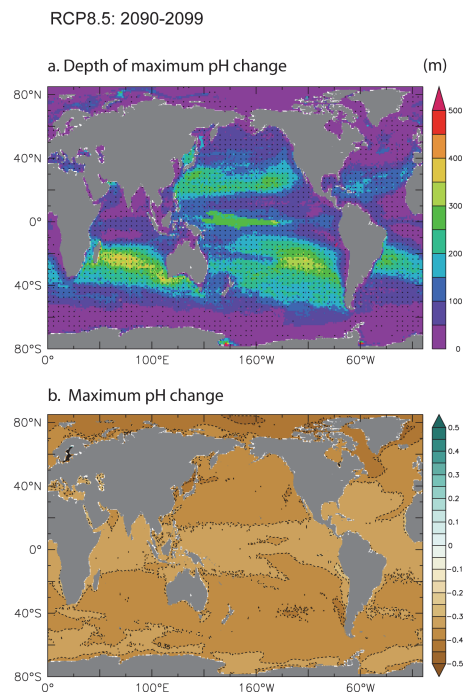


Fig. 7. Change in pH in 2090–2099 relative to 1990–1999 under RCP8.5. (a) Model-mean depth of the maximum changes in pH. Robustness estimated from inter-model standard deviation and (b) model-mean changes of pH at that depth.

3670

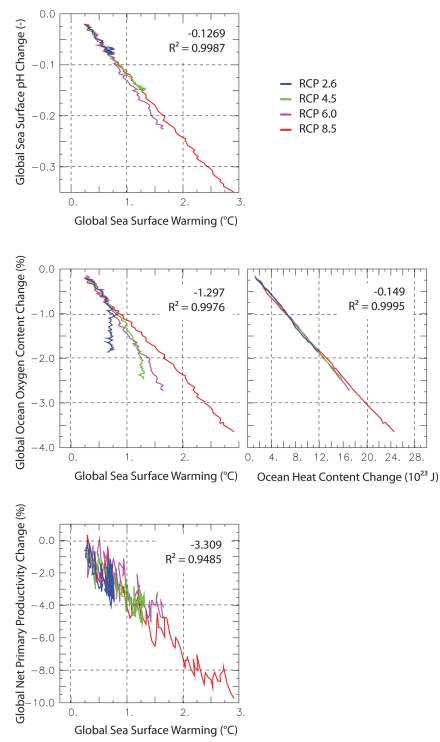


Fig. 10. Relations between model-mean changes in surface pH (pH unit), global O₂ content (%) and global NPP and model-mean sea surface warming (°C) for all scenarios. For global O₂ content, changes are also plotted against changes in total heat content (10²²J). All changes are relative to 1990–1999 and plotted over 2006–2100.

3673

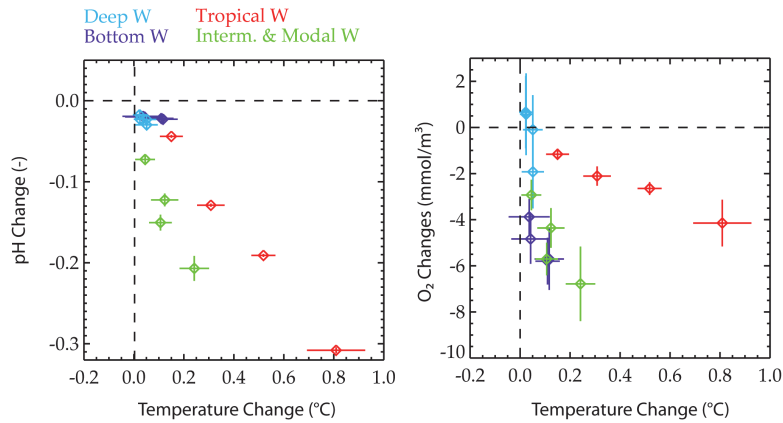


Fig. 11. Relations between model-mean changes in pH (pH unit), dissolved O₂ (mmol m⁻³) and model-mean temperature change (°C), in four distinct global water masses (tropical water mass, modal and intermediate water mass, deep water mass and bottom water mass). For a definition of the different water masses, please see Sect. 2.3. Inter-model standard deviations are also indicated.

3674

